2 Physics at a Symmetric 10^{33} e^+e^- Collider

In this chapter we discuss the physics goals using the CESR Phase 3 symmetric e^+e^- collider, capable of producing a peak luminosity of $1--2\times10^{33}\text{cm}^{-2}\text{sec}^{-1}$ at the $\Upsilon(4S)$. At this luminosity, the program will cover all aspects of heavy quark and tau lepton physics with high precision; the CLEO III experiment will continue to be at the very forefront of testing and understanding the Standard Model and beyond. Measurements of rare decays and form factors, precision measurements of the CKM parameters V_{cb} and V_{ub}, and the possibility that CP violation may be observed in the B system are just some of the crucial and exciting physics prospects.

To quantitatively evaluate the physics possibilities, we first make some assumptions about the future performance of CESR. We assume that CESR Phase 3 will have provided integrated luminosities of 20 fb^{-1} on the $\Upsilon(4S)$ resonance and 10 fb^{-1} on nearby continuum within a few years after commissioning. This comes after our projection that CLEO II will have accumulated 5 fb^{-1} of integrated luminosity and half that amount off the peak during CESR Phase 2. The physics program of CLEO III will have the advantage of an improved detector with excellent charged hadron identification and precision vertex information. The CLEO III detector thus provides the new tools necessary to probe rare processes and extract most of the important new results we foresee. The following sections outline the topics in which precision can be improved or new discoveries can be made.

2.1 B decay studies

2.1.1 Goals of B decay studies

Does the Standard Model explain quark mixing?

There are presently two fundamental questions in the forefront of high energy physics. One concerns the origin of mass which revolves around the scalar sector. This is being pursued in Higgs particle searches at super-high energies at Fermilab and CERN. The other equally deep and probably related question concerns the origin of quark mixing and, thus, CP violation. CLEO III with its unique ability to measure rare processes is in a position to pursue this question by performing redundant measurements of the unitary triangle shown in Fig. 4. These measurements couple our studies with the important question of baryon-antibaryon asymmetry in the universe and thus with the very reasons that we may exist.

The unitary triangle is depicted in a two dimensional space where the Wolfenstein[4] parameters ρ and η form the horizontal and vertical axes. The sides and angles of the triangle are directly related to physical measurements. One side is proportional to the absolute value of the ratio of CKM elements V_{ub}/V_{cb}. This can be measured by observing the relative yields of $b\to u$ versus $b\to c$ in specific processes, such as semileptonic decay.

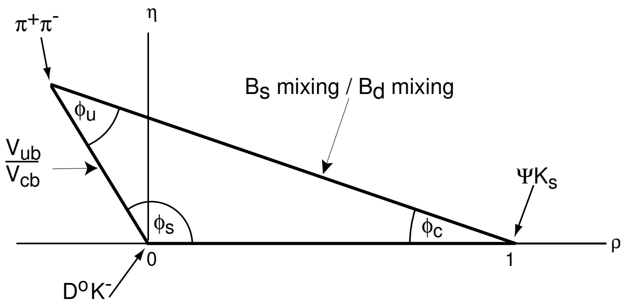

Figure 4: The unitary triangle shown in ρ vs. $i\eta$ space.

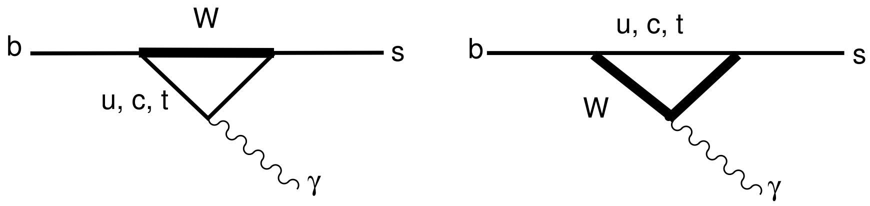

Figure 5: Radiative penguin diagrams.

Another side is proportional to the ratio V_{td}/V_{ts} which can be inferred by measuring the ratio of mixing rates for B_s^0 and B_d^0 or by measuring the ratio of widths $\Gamma(B \to \rho\gamma)/\Gamma(B \to K^*\gamma)$. The three angles of the triangle can be found by measuring CP violation in three different types of B decay. Typical modes are shown in Fig. 4. Whereas the angles ϕ_c and ϕ_u can be determined at the $\Upsilon(4S)$ with an asymmetric collider, the angle ϕ_s can be discovered with a symmetric machine using charged B decays. Additional information constraining the unitary triangle is available from other measurements including ϵ and ϵ'/ϵ in kaon decay and B_d mixing, but these typically have two problems associated with their interpretation: they are functions of the unknown top quark mass and the hadronic matrix elements that relate the CKM parameters to the measurements need to be calculated theoretically. The measurements of the sides of the triangle have the latter problem, although to a lesser extent.

Physics beyond the Standard Model

B mesons can decay via loop diagrams which are sensitive to new physics, as well as physics predicted by the Standard Model. The existence of one such class of diagrams, called "penguins," was predicted to explain the Δ I = 1/2 rule in kaon decays[5].

In Fig. 5 we show the Feynman diagram for the penguin process. Such decays have recently been established in CLEO II with evidence for the exclusive channel $B \to K^*\gamma$[1]. The study of radiative penguin processes, in particular measurements of the inclusive radiative penguin rate, $b \to s\gamma$, are important for setting constraints on models beyond the Standard Model. As the accumulated luminosity increases, the study of the exclusive penguin process will become viable as will the search for other non-standard processes such as $B \to K\mu e$.

Table 1: Form-factor ratios at q^2_{max} from CLEO. The q^2 dependence used in the fits of the data has been assumed to follow the models indicated.

	A_2/A_1	V/A_1	$\|V_{cb}\|A_1$
Data fit for ISGW	1.02 ± 0.24	1.07 ± 0.57	$0.035 \pm 0.003 \pm 0.002$
Data fit for HQET*	0.79 ± 0.28	1.32 ± 0.62	$0.037 \pm 0.003 \pm 0.002$
ISGW[7]	1.14	1.27	
KS[8]	1.39	1.54	
WSB[9]	1.06	1.14	
HQET	1.26	1.26	
HQET*	1.14	1.74	

QCD physics

Although the study of weak decays of b-quarks is the primary motivation for CLEO III, the b-quark is probably the only laboratory to study Quantum Chromodynamics (QCD) in heavy quark systems. The charm quark is probably too light to show the asymptotic behavior expected in Heavy Quark Effective Theory[6] (HQET) and the top quark is too heavy to form mesons prior to its decay. Moreover, a thorough understanding of QCD effects is necessary to extract the fundamental CKM parameters V_{cb} and V_{ub} with precision.

2.1.2 V_{cb} and form-factors in semileptonic decays

In purely hadronic B decays the virtual W from the $b \to c$ (or $b \to u$) transition materializes as a quark-antiquark pair. In addition, the spectator-antiquark participates in the decay process. The result is a 4-quark system that can interact in a myriad of ways via the exchange of gluons. In such a system, predictions of branching fractions or even ratios of branching fractions are difficult. In semileptonic decays the virtual W materializes as $\ell^- \bar{\nu}_\ell$ and thus only the c-quark (or u-quark) spectator-antiquark system needs to be modeled. Thus, semileptonic B decays provide the best opportunities for measurement of the CKM parameters V_{cb} and V_{ub}. For V_{cb} CLEO has shown that an excellent procedure is to use the channels $\bar{B}^0 \to D^{*+}\ell^-\bar{\nu}_\ell$ and $B^- \to D^{*0}\ell^-\bar{\nu}_\ell$. These exclusive channels are selected by calculating the missing mass squared recoiling against the observed D^* and ℓ^-. Missing mass distributions from the CLEO II data for these decays are shown in Fig. 6. Thus far, form-factor ratios have been inferred from the data and they are given in Table 1.

It is important to measure both the q^2 dependence and the values of the form-factors at q^2_{max} in order to compare with HQET and to extract values of V_{cb}. HQET predicts one universal form-factor function, dependent on q^2 and absolutely normalized at $q^2 = q^2_{max}$, which describes all $B \to D^*(D)\ell\bar{\nu}$ decays[10]. One can take advantage of HQET to measure

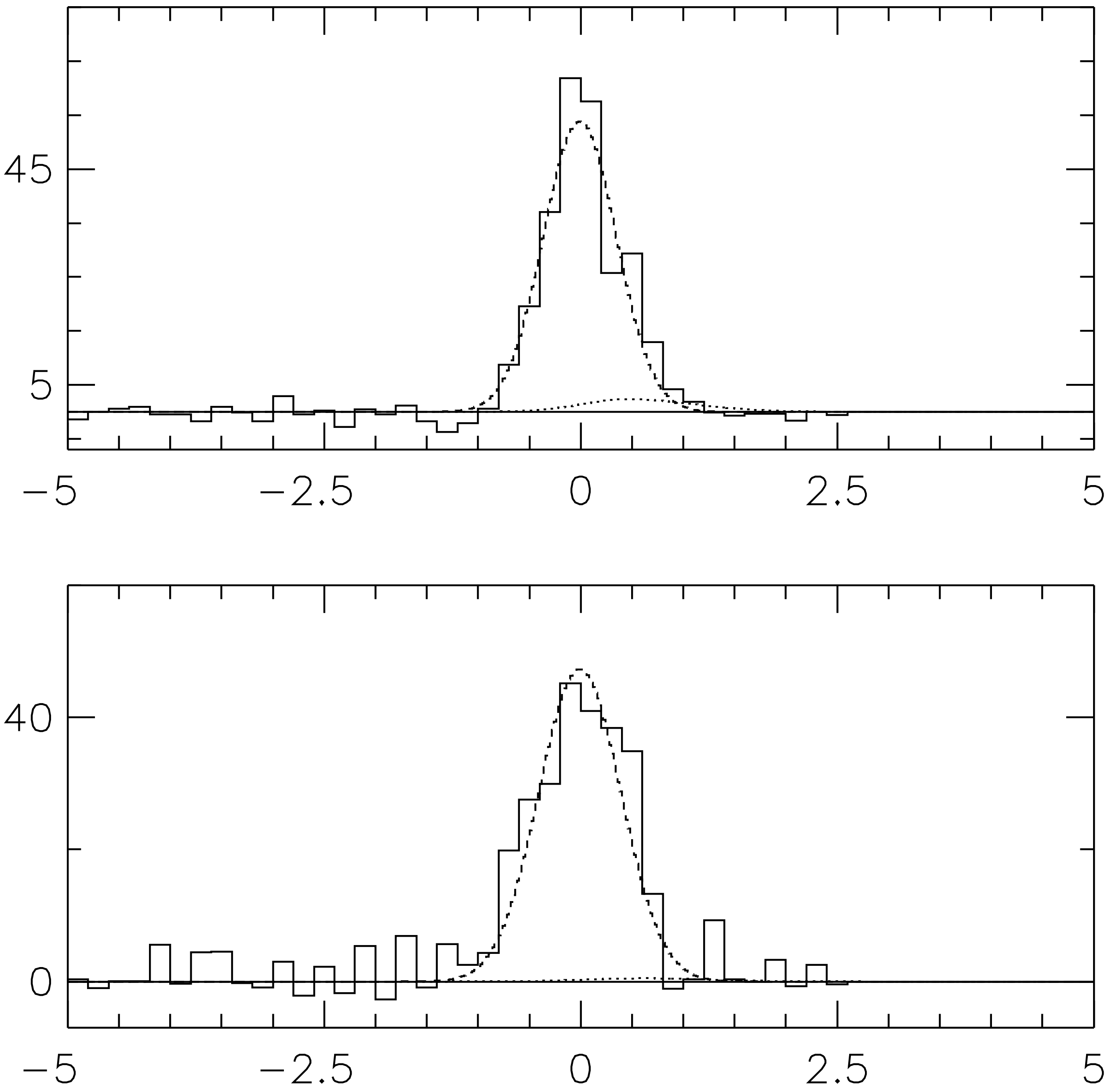

Figure 6: Signals for $D^{*+}\ell\nu$ (top) and $D^{*0}\ell\nu$ (bottom) from CLEO II. All combinatoric backgrounds have been subtracted. The histogram is the data, the dashed line is the $D^{*}\ell\nu$ signal and the dotted line $D^{**}\ell\nu$ signal from a fit to the data.

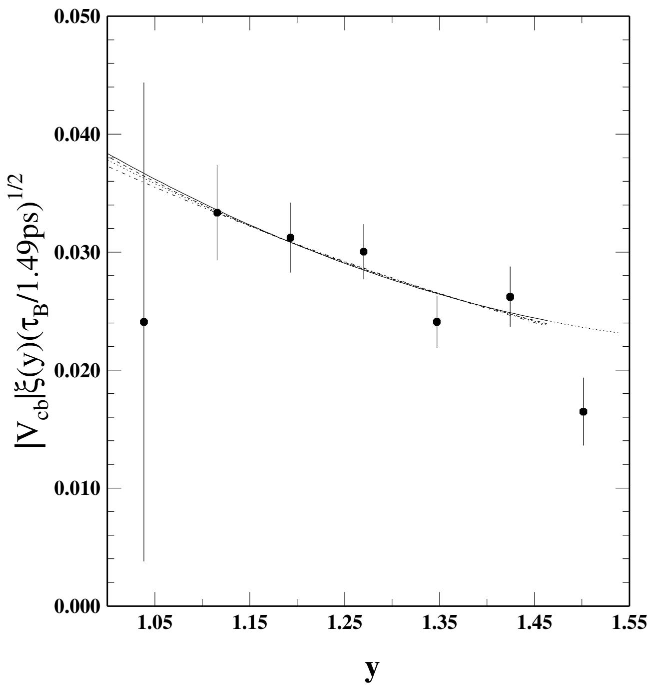

Figure 7: $(\tau_B/1.49ps)^{1/2}|V_{cb}|\xi(y)$ versus y extracted from CLEO II data for $\bar{B}^0 \to D^{*+}\ell^-\bar{\nu}_\ell$.

V_{cb} by extrapolating the q^2 dependence of $\frac{d\Gamma}{dy}(B \to D^*\ell\nu)$ to q^2_{max} as shown in Fig. 7. The intercept at q^2_{max} yields V_{cb}. Note, $y = (m_B^2 + m_{D^*}^2 + -q^2)/2m_B m_{D^*}$ and $y(q^2_{max}) = 1$.

One problem with this analysis is the background from the D^{**} (or $D^*\pi$) final states. This background can be eliminated by using only events with negative missing mass squared. This, however, results in a loss of half the signal. Improvements in background rejection are clearly necessary. Good charged particle identification will improve the D^* signal; vertex detection can be used to reduce backgrounds by requiring that the D and the ℓ^- form an acceptable B vertex.

2.1.3 Rare B decays

Precision measurement of V_{ub}

Thus far the only evidence for the $b \to u$ transition has been in the observation of leptons with momenta above that allowed for $b \to c$ transitions. Recent measurements from CLEO II show somewhat smaller signals than reported originally[11]. Figure 8 shows the CLEO II signal and Table 2 provides a summary of recent measurements. The extracted values of V_{ub}/V_{cb} are based on the Altarelli model[12], with the results of different models differing by more than $\pm$ 50%.

CLEO has searched for evidence of the exclusive semileptonic reactions $B \to \rho(\omega)\ell^-\bar{\nu}_\ell$, for which ARGUS has claimed an observation[15]. CLEO does not observe these final states and quotes an upper limit $\mathcal{B}(B^- \to V^0\ell^-\bar{\nu}_\ell) < (1.6--2.7)\times 10^{-4}$ at the 90% confidence level[16].

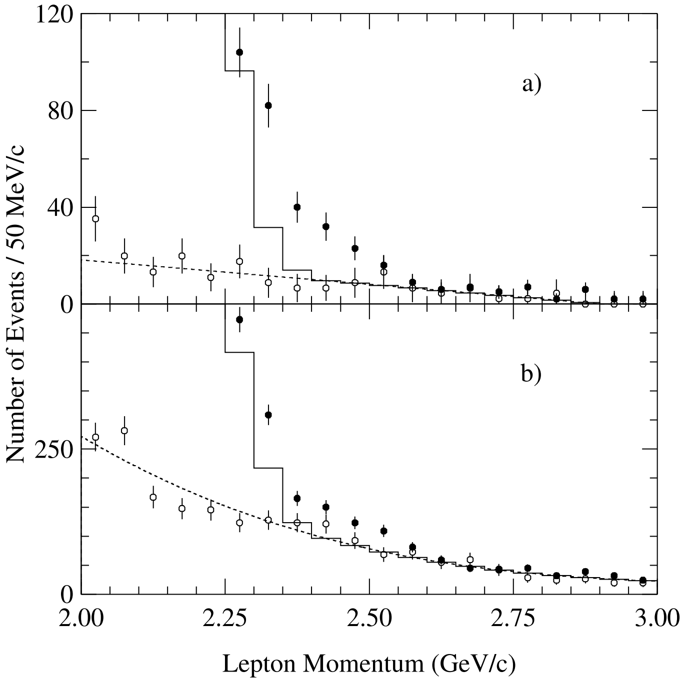

Figure 8: Lepton endpoint spectrum from CLEO II after a) a strict and b) an $R_2 < 0.3$ continuum-suppression cut has been applied. The data represent the sum of electrons and muons. The filled points are data on the $\Upsilon(4S)$ while the open points are scaled continuum data. The dashed curves are fits to the off-resonance data and the solid curves show the predicted $b \to c\ell\nu$ contribution added to the fits of the off-resonance data.

Table 2: Summary of V_{ub}/V_{cb} measurements in Altarelli model

Experiment	V_{ub}/V_{cb}
CLEO 90[13]	0.100±0.015
ARGUS 90[14]	0.10 ±0.01
CLEO 92	0.075±0.008

The range of values reflects differences in theoretical models (see Fig. 9). With twenty times the statistics expected from the CESR upgrade and the addition of background reduction supplied by particle identification and vertex detection, we should be able to measure the branching ratios, but probably not the form-factors.

Theoretical input on these crucial B decay parameters may be obtained from applying HQET to the corresponding charm decays $D \to \rho(\omega)\ell^+\nu_\ell$, which CLEO III can measure, and possibly from studies of $b \to s\gamma$.

Measurement of "penguin" processes

Radiative b decays can occur only via the "penguin" diagrams shown in Fig. 5. The simplest such decay is $B \to K^*\gamma$, since the decay $K\gamma$ is forbidden by angular momentum conservation. CLEO has recently made the first observation of this process[1]. The data are shown in Fig. 10 and the measured branching ratio is $(4.5 \pm 1.5 \pm 0.9) \times 10^{-5}$.

There are also hadronic penguins. The diagrams for these processes can be obtained by replacing the photon with a gluon. Examples of such processes are $\bar{B}^0 \to K^-\pi^+$ and the Cabibbo-suppressed decay $\bar{B}^0 \to \pi^+\pi^-$[17]. Interference between the rare "penguin" processes and the $b \to u$ transitions may provide a means of seeing CP violation in B decays. CLEO has recently shown evidence that these processes do exist[18].

The Standard Model requires penguins to explain K decay and predicts B decays that occur only via penguins to have branching ratios in the 10^{-5} range. The inclusive branching ratio $\mathcal{B}(b \to s\gamma)$ is predicted to be $\sim 4{\times}10^{-4}$[19]. The shape of the inclusive hadronic mass spectrum[20] (see Fig. 11) and exclusive branching ratios[21] (see Table 3) have also been calculated. Measuring the branching ratios for explicit channels determines values of the form-factors at $q^2{=}0$. These are intimately related to the form-factors in $b \to u$ exclusive semileptonic decays and thus may be useful in pinning them down.

Another exciting possibility is to determine the length of one side of the CKM triangle by measuring the penguin process $B \to \rho\gamma$. This, when combined with $\mathcal{B}(B \to K^*\gamma)$, could

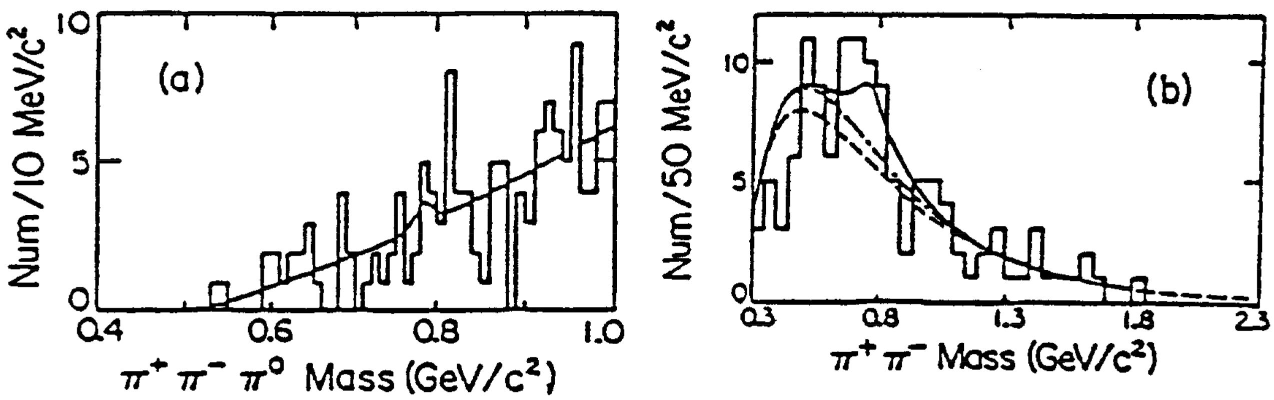

Figure 9: Invariant mass spectra for searches for (a) ω and (b) ρ in exclusive semileptonic decays from CLEO.

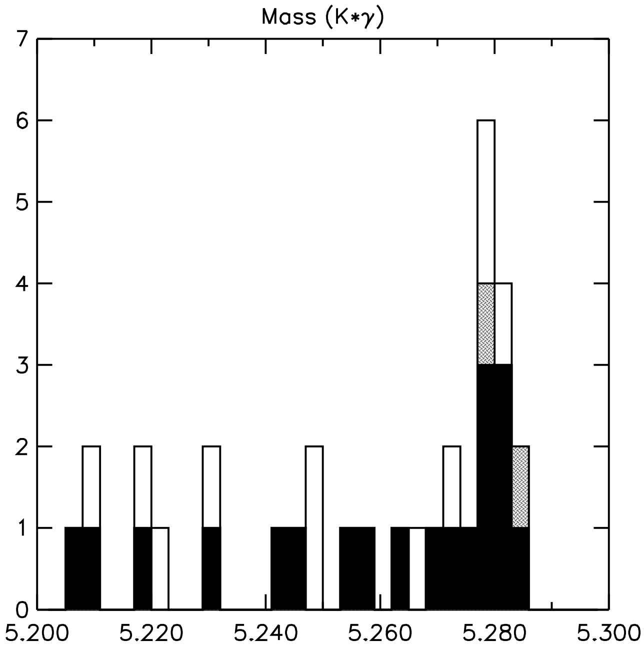

Figure 10: The B candidate mass spectrum for $K^*\gamma$ final states. The final states are coded as follows: shaded, $K_S\pi^-$; solid, $K^-\pi^+$; and open, $K^-\pi^0$.

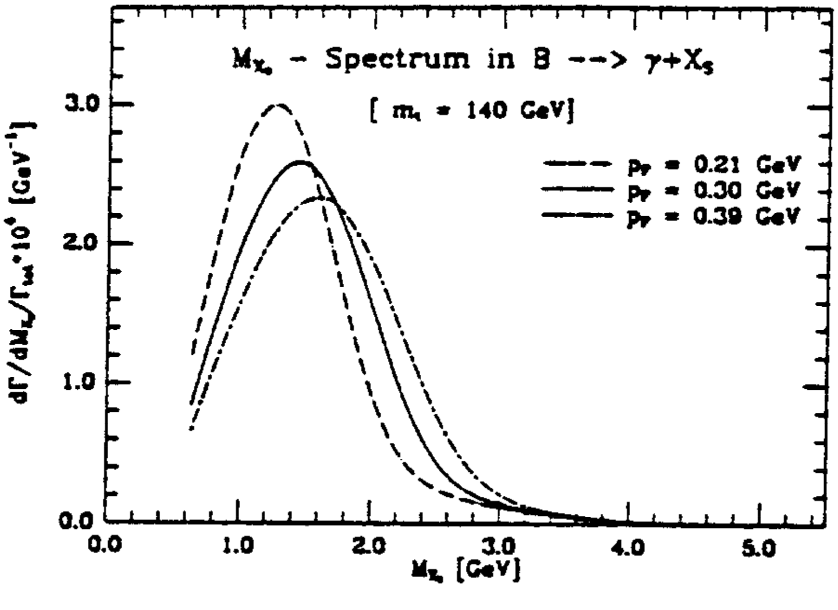

Figure 11: Predicted mass spectra of $b \to s\gamma$ from Ali and Greub[20].

Table 3: Exclusive radiative penguin rates

Name	J^P	$\mathcal{B}(B \to K^*\gamma)/\mathcal{B}(B \to s\gamma)$	$\mathcal{B} \times 10^5$
K	0^-	forbidden	forbidden
$K^*(890)$	1^-	(3.5–12.2)%	1.4–4.9
$K^*(1410)$	1^-	(7.2–10.6)%	2.9–4.2
$K^*(1680)$	1^-	(1.1–1.5)%	0.4–0.6
$K_2(1580)$	2^-	(4.5–6.4)%	1.8–2.6
$K^*(1430)$	0^+	forbidden	forbidden
$K^*(1270)$	1^+	(4.5–10.1)%	1.8–4.0
$K_1(1400)$	1^+	(6.0–13.0)%	2.4–5.2
$K_2^*(1430)$	2^+	(17.3–37.1)%	6.9–14.8
Sum		(44.1–90.9)%	17.6–36.6

be used to determine the ratio V_{td}/V_{ts}. Clearly, charged hadron identification is essential to distinguish the ρ from the K^* and it also very useful in reducing backgrounds in all of the rare decay channels.

As an illustration of the sensitivity of the penguin process to high mass objects beyond the Standard Model we show in Fig. 12 the implications for the two Higgs doublet model. In such a model a charged Higgs boson $H^\pm$ can substitute for the $W^\pm$ in the loop. The figure shows the region in the space of mass m_H versus ratio of vacuum expectation values $\tan\beta$ that is consistent with the CLEO II limits on $b \to s\gamma$ branching ratio. Masses less than 250 GeV/c^2 are excluded for this model.

Another example is the search for a supersymmetric squark. Figure 13 shows the region in the squark mass versus Higgs mass space[26] excluded by the CLEO II $b \to s\gamma$ limits. Only the range $\tilde{m}/m_H > 1$ is excluded.

Higher luminosity will increase the sensitivity to more loop decays and will allow a more precise comparison with Standard Model predictions, thus improving our sensitivity to high mass extensions or violations of the Model. This opens a window to new physics that is competitive with the much more expensive approach of building higher energy colliders.

The recent CLEO II observation of the sum of $\bar{B}^0 \to K^-\pi^+$ and $\bar{B}^0 \to \pi^-\pi^+$ mentioned above [2] is consistent with a $K\pi$ loop decay branching ratio, $(1.1 \pm 0.7) \times 10^{-5}$. With the CESR/CLEO upgrade this measurement will improve as a result of the increased luminosity and the new high momentum particle identification system. Also we can expect many other $b \to sg$ loop decay modes to show up. Table 4 shows some of the theoretical predictions.

Decays to baryon-antibaryon pairs

The B can decay to baryons and, therefore, offers a unique opportunity to study the

Table 4: Predictions for some exclusive hadronic loop decays

Mode		$\mathcal{B}(10^{-5})$[22]	$\mathcal{B}(10^{-5})$[23]
$\bar{B}^0 \to$	$K^-\pi^+$	1.8	2.5
	$\bar{K}^0\pi^0$	0.7	
	$\bar{K}^0\phi$	1.5	
	$K^{*-}\pi^+$	1.8	2.2
	$K^{*-}\rho^+$	1.6	2.7
	$\bar{K}^{*0}\rho^0$	0.8	
	$\bar{K}^{*0}\phi$	4.2	
$B^- \to$	$K^-\pi^0$	1.2	1.2
	$\bar{K}^0\pi^-$	1.4	
	$K^-\phi$	1.5	1.5
	$K^{*-}\pi^0$	0.9	
	$\bar{K}^{*0}\pi^-$	0.8	
	$K^{*-}\rho^0$	0.8	1.4
	$\bar{K}^{*0}\rho^-$	1.6	
	$K^{*-}\omega$		1.3
	$K^{*-}\phi$	4.2	2.1

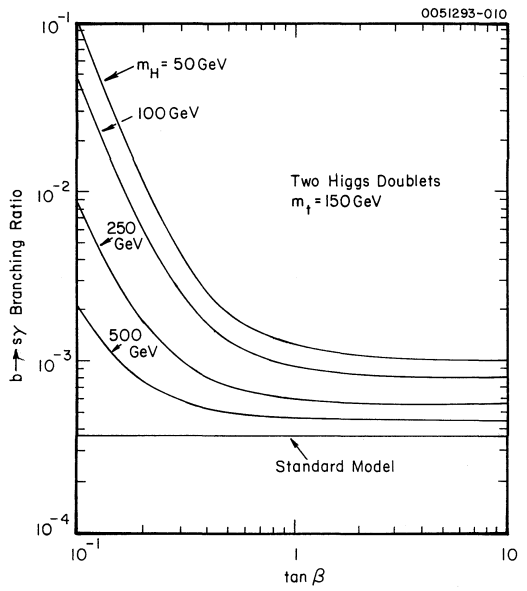

Figure 12: Predictions of the branching ratio $\mathcal{B}$ for $b \to s\gamma$ in the two Higgs doublet model[24], for various values of Higgs mass and the ratio $\tan\beta$ of vacuum expectation values, with the top mass assumed to be 150 GeV/c^2. CLEO II measurements[25, 1] allow $0.5 \times 10^{-4} < \mathcal{B} < 5.4 \times 10^{-4}$.

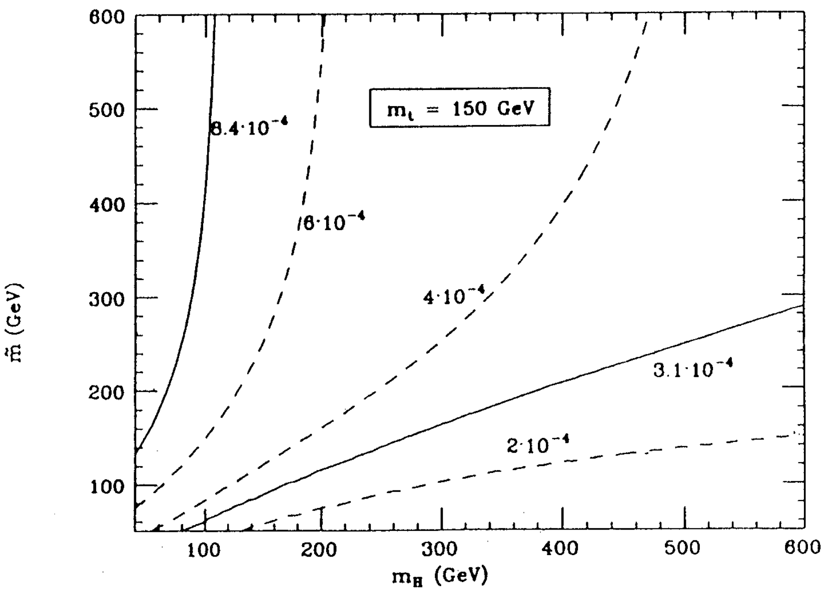

Figure 13: Predicted branching ratio for $b \to s\gamma$ (the labels on the curves) assuming a supersymmetric squark of mass $\tilde{m}$ and a Higgs boson of mass m_H [26] for a top quark mass of 150 GeV/C^2. The CLEO II data[1, 25] allow $0.5 \times 10^{-4} < \mathcal{B} < 5.4 \times 10^{-4}$.

dynamics of baryon pair creation in a reaction where at least the initial state and the initial coupling are well defined. Even at the most fundamental level we are completely ignorant of the production mechanism. For example, does it proceed through diquark-antidiquark pairs? There are data from CLEO and ARGUS on inclusive proton, Λ, and Λ_c yields in B decay [27] but because of the low efficiencies for reconstructing exclusive decays of B mesons and charmed baryons, a definitive study must await the larger data samples from the upgraded CESR.

Purely leptonic decays

In the Standard Model the purely leptonic decay of the B into a lepton and a neutrino should proceed as in pion decay, through the annihilation of the b and $\bar{u}$ quarks into a W^-, materializing as $\ell^- + \bar{\nu}$. The rate is proportional to $|V_{ub}|^2$ and to the $b\bar{u}$ bound-state overlap factor f_B^2. Once V_{ub} is known, a measurement can give us an experimental value for f_B, which comes into calculations of mixing, CP violation, and other weak processes involving the interaction between the quarks in the B meson. Theoretical predictions for f_B from QCD sum rules[28] and lattice calculations[29] cover the range from 105 to 187 MeV.

The leptonic decay rate is also sensitive to new physics; for example, the mass $m_{t\pi}$ and coupling λ of a possible technipion can be limited [30] by

$$\frac{m_{t\pi}}{\lambda} = 200 \text{ GeV} \left(\frac{10^{-6}}{\mathcal{B}(B \to \tau\bar{\nu})} \right)^{1/4} .$$

Since the rate should be proportional to the square of the lepton mass, the most copious mode is $B \to \tau\bar{\nu}$, which however is identifiable only in tagged $B\bar{B}$ events, because of the missing neutrinos. The much smaller branching ratio for $B \to \mu\bar{\nu}$, about 10^{-7}, might be measurable without tagging, since the muons will be nearly monoenergetic near the $B\bar{B}$ threshold. Very high luminosities may be required, however, since a B branching ratio of 10^{-7} yields only about one event per 10 fb^{-1} at the $\Upsilon(4S)$. Non-Standard Model enhancements, however, could give a much larger event rate.

Forbidden dilepton decays

Certain B decays are strictly forbidden in the Standard Model, for example, those that violate an accepted conservation law. Still other decays may be allowed but at an undetectably low branching ratio. In the cases in which the particular final state is easily recognizable experimentally and not obscured by backgrounds, the search for such modes can expose weaknesses in the model. Typical examples are $B \to \mu e$ and $B \to \tau\mu$, which are forbidden by the absence of transitions between lepton families in the Standard Model. If there were a "horizontal gauge boson" H^0 that would allow $b\bar{d} \to H^0 \to \mu e$, the branching ratio for $B \to \mu e$ would be[31]

$$130 \left(\frac{m_W}{M_H}\right)^4 \left(\frac{f_B}{100\ \mathrm{MeV}}\right)^2 .$$

The present CLEO[32] upper limit of 5.9×10^{-6}, limited only by the size of the available event sample, implies a lower limit on the mass of the horizontal gauge boson of 8 TeV. The mass sensitivity increases as the fourth root of the number of B decays searched.

The decays $B \to e^+e^-$ and $B \to \mu^+\mu^-$ violate the Standard Model GIM suppression of flavor changing neutral currents, but are allowed through loop diagrams at the level of 10^{-12} and 10^{-8} respectively[33]. The CLEO upper limits, 5.9×10^{-6} for both[32], can be improved simply by searching larger data samples.

2.1.4 CP violation

Possibilities for observing CP violation and measuring ϕ_s

Gronau and Wyler[3] have proposed a method of measuring ϕ_s using only measured branching fractions in charged B decay[34]. The method is best illustrated by considering the three related B^- decay modes, and the corresponding modes for B^+, $B^- \to D^0K^-$, $B^- \to \bar{D}^0K^-$, and $B^- \to D_{CP}K^-$, where D_{CP} indicates that the D^0 decays into a CP eigenstate. The weak decay diagrams[35] for the first two modes are shown in Fig. 14. The first decay is a Cabibbo-suppressed version of $B^- \to D^0\pi^-$, while the second is a color suppressed $b \to u$ transition where the virtual W^- transforms itself into a $\bar{c}s$ pair.

Interference is possible between the two decay modes if the D^0 decays into a non-strangeness specific mode. Examples of such final states include K^+K^-, $K_S\pi^0$, and $K_S\pi^+\pi^-$. To simplify the discussion, we only use such states which are in specific angular momentum configurations so that their CP is defined as +1 or -1; these states are usually denoted as

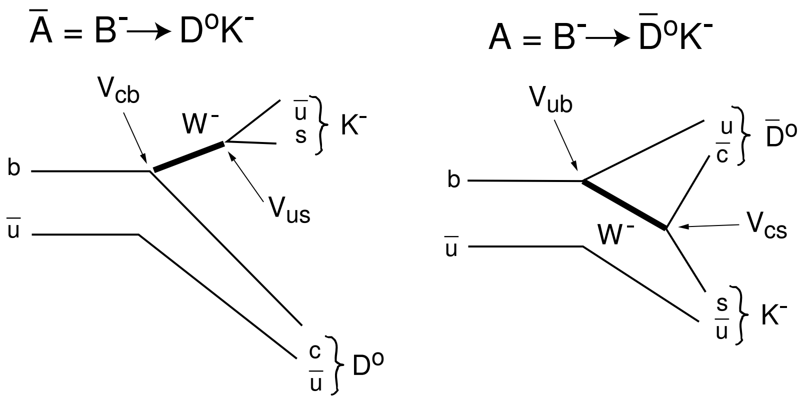

Figure 14: Quark level decay diagrams for $B \to DK^-$.

D^0_1 and D^0_2. We have that

$$D^0_1 = \frac{1}{\sqrt{2}}\left[D^0 + \bar{D}^0\right], \quad \text{and} \quad D^0_2 = \frac{1}{\sqrt{2}}\left[D^0 - \bar{D}^0\right].$$

To further simply the discussion we will consider only D^0_1's. The amplitudes for the relevant $B^\pm$ decay modes are related by

$$\sqrt{2}A^+_1(B^+ \to D^0_1 K^+) = A(B^+ \to \bar{D}^0 K^+) + A(B^+ \to D^0 K^+) \tag{6}$$
$$\sqrt{2}A^-_1(B^- \to D^0_1 K^-) = A(B^- \to \bar{D}^0 K^-) + A(B^- \to D^0 K^-). \tag{7}$$

The branching fractions for the decays $B^+ \to D^0_1 K^+$ and $B^- \to D^0_1 K^-$ need not be equal and a difference between them would be a manifest demonstration of CP violation in charged B meson decay. Two amplitudes are equal in magnitude,

$$|A| \equiv |A(B^+ \to D^0 K^+)| = |A(B^- \to \bar{D}^0 K^-)| \tag{8}$$
$$|\bar{A}| \equiv |A(B^+ \to \bar{D}^0 K^+)| = |A(B^- \to D^0 K^-)|. \tag{9}$$

Then denoting the relative hadronic phase between the amplitudes A and $\bar{A}$ by δ[37] we have

$$\sqrt{2}A^+_1 = |A|e^{i(+\phi_s+\delta)} + |\bar{A}| \tag{10}$$
$$\sqrt{2}A^-_1 = |A|e^{i(-\phi_s+\delta)} + |\bar{A}|. \tag{11}$$

To determine ϕ_s we need to measure the branching fractions for the modes in Eqs. 6 and 7. Two triangles are constructed from the square roots of the branching fractions as illustrated in Fig. 15. The angles ϕ_s and δ are then determined.

This method leads to a four-fold ambiguity in the value of $\sin\phi_s$. Half the ambiguity is removed if one uses the measurement of ϵ in K^0 decay which leads to the boundary condition $\sin\phi_s > 0$. The other ambiguity arises between the determination of ϕ_s and δ. This ambiguity can be removed by measuring other related decay modes, such as $B^- \to D^{*0}K^-$, which are likely to have a different strong phase shift δ but must have the same CP violating phase. It

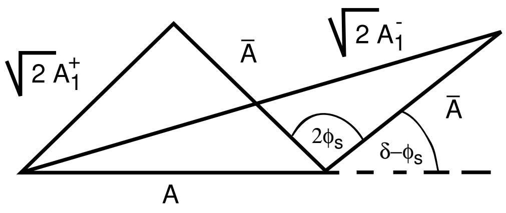

Figure 15: The two triangles constructed out of the four different measured rates and the phase relationships between the two triangles.

is also important to realize that this method can find a value for ϕ_s even if δ is zero. In this case the two triangles for B^- and B^+ are congruent.

Observation of CP asymmetry is expedited by having comparable amplitudes for the two interfering decays. At the CKM level (ignoring color suppression), the magnitude of the amplitude $\bar{A}$ is $V_{cb}V_{us} = a\lambda^3$, while the magnitude of the amplitude A is $|V_{ub}|V_{cs} \approx (|V_{ub}/V_{cb}|)V_{cb} \approx 0.08a\lambda^2$ where a and λ are the parameters defined by Wolfenstein[4, 38, 39]. Therefore at the CKM level the ratio of the amplitudes is $|A/\bar{A}| \approx 0.08/\lambda \approx 1/3$. However, $\bar{A}$ occurs through a color-allowed diagram while the diagram for A is color-suppressed. However, there is a simple way to predict the branching fraction corresponding to the amplitude A. Consider the measured decay mode, $B^- \to \psi K^-$, which is very similar to the mode $B^- \to \bar{D}^{*0}K^-$. The decay diagrams are shown in Fig. 16. The difference between the two diagrams is that the ψ decay occurs when there is a $b \to c$ transition, while the $\bar{D}^{*0}$ occurs when there is a $b \to u$ transition. We choose to discuss $\bar{D}^{*0}$ here rather than $\bar{D}^0$ since $\bar{D}^{*0}$ is a vector meson as is the ψ. Correcting for phase space effects we have

$$\mathcal{B}(B^- \to \bar{D}^{*0}K^-) = \mathcal{B}(B^- \to \psi K^-)\left|\frac{V_{ub}}{V_{cb}}\right|^2 \left(\frac{f_{D^*}}{f_\psi}\right)^2 \cdot P, \tag{12}$$

where P is a phase space factor equal to 1.3, and the f's are form-factors. These form-factors are not known; theoretical predictions give $(f_{D^*}/f_\psi)^2 \approx 50\%$[45]. Using $\mathcal{B}(B^- \to \psi K^-) \approx 1.1 \times 10^{-3}$[41], the prediction is that $\mathcal{B}(B^- \to \bar{D}^{*0}K^-) = (4.8 \pm 2.7) \times 10^{-6}$. The error comes from the uncertainty on the ψK^- branching ratio and the uncertainty in V_{ub}/V_{cb}. A similar prediction can be made for the $\bar{D}^{*0}K^{*-}$ final state and is listed in Table 5.

The final states with a scalar D^0 rather than a vector D^{*0} are more difficult to predict because the analogous $b \to c$ mode, $\eta_c K$, has not been observed, nor are there any upper limits. There are two theoretical predictions that inclusive η_c modes are half the ψ modes[40]. The estimates given in Table 5 use the assumption that is also true for the exclusive modes. For the sum of branching ratios we use a value of 18×10^{-6} for subsequent estimates.

To estimate the branching fraction $\mathcal{B}(B^- \to D^0K^-)$ with amplitude of type $\bar{A}$, we take the new CLEO measurement[41] $\mathcal{B}(B^- \to D^0\pi^-) \approx 0.47\%$ and multiply it by the Cabibbo suppression factor λ^2 and the enhancement factor $(f_K/f_\pi)^2 \approx 1.5$[42]. The result is $\mathcal{B}(B^- \to D^0K^-) \sim 3.3 \times 10^{-4}$.

In a 20 fb^{-1} data sample, the expected number of events is given by the product of

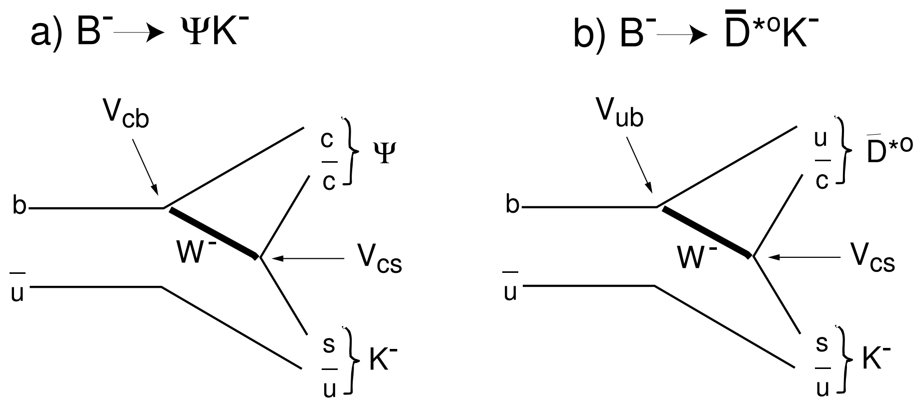

Figure 16: Decay diagrams for (a) $B^- \to \psi K^-$ and (b) $B^- \to \bar{D}^{*0} K^-$.

Table 5: Branching ratio estimates for $B^- \to \bar{D}K^-$ modes (with amplitudes of type A).

B^- Mode	$\mathcal{B}$
$\bar{D}^0 K^-$	2.4×10^{-6} †
$\bar{D}^{*0} K^-$	$(4.8 \pm 2.7) \times 10^{-6}$
$\bar{D}^0 K^{*-}$	3.5×10^{-6} †
$\bar{D}^{*0} K^{*-}$	$(7.0 \pm 4.3) \times 10^{-6}$
Sum	$\sim 18 \times 10^{-6}$

† This estimate is half the corresponding rate with a $\bar{D}^{*0}$.

Table 6: CP eigenstate modes of D^0 decay.

mode	$\mathcal{B}(\%)$	ϵ	$\mathcal{B} \times \epsilon(\%)$
K^+K^-	0.5	0.74	0.37
$K_S\omega$	1.9	0.09	0.16
$K_S\pi^0$	1.4	0.15	0.21
$K_S\eta'$	1.0	0.04	0.04
$K_S\phi$	0.4	0.18	0.07
$K_S\eta$	0.4	0.07	0.03
$K^{*0}\pi^{0\dagger}$	0.8	0.10	0.08
$\pi^+\pi^-$	0.2	0.74	0.15
SUM			1.11

† The branching ratio is only for the $K_S\pi^0$ decay.

several factors, including the integrated luminosity, the $\Upsilon(4S)$ cross section (1 nb), the $\bar{D}^0$ detection efficiency (0.09), the efficiency for finding a single charged pion (0.9), and other cuts used to enhance signal to background. The $\bar{D}^0$ detection efficiency is calculated using the three modes $K^-\pi^+$, $K^-\pi^+\pi^0$, and $K^-\pi^+\pi^+\pi^-$. The cuts used to enhance the signal to background include a cut on the momentum direction of the B candidate compared with the thrust axis of the rest of the event. These have an efficiency of 80%. This gives a total of 400 such events summed over B^- and B^+ decays[43]. We can add other decay modes, although the analysis must be carried out for them individually because of the ambiguity between ϕ_s and δ in each mode. Using more than one mode provides a way of resolving this ambiguity. The other obvious final states are $\bar{D}^{*0}K^-$, $\bar{D}^0K^{*-}$, and $\bar{D}^{*0}K^{*-}$. Summing all of these modes leads to approximately 1600 events. The number of type A decays, based on the summed branching ratio of 18×10^{-6}, is 20. These rate estimates may be conservative in that they use the current CLEO II efficiencies.

The CP eigenstate decay modes are more prolific. Table 6 shows that the branching ratio times efficiency for these decays is approximately 10% of that of the D^0 decays used above.

In order to evaluate how accurate a measurement of sinϕ_s can be made with 20 fb^{-1}, we use the expression given by Gronau and Wyler[3] for determining $\sin\phi_s$ from $|A|$, $|\bar{A}|$, and $|A_1^{\pm}|$. The numbers of events going through the channels $\bar{A}$ and A have been taken to be 800 and 20. (The use of 800 rather than 1600 events is based on lower measurements of type $\bar{A}$ than are currently available; this change is not expected to significantly affect the accuracy of the measurement.) Choosing values for ϕ_s and δ defines the number of events in the A_1^+ and A_1^- channels. These latter values are calculated applying the law of cosines to the triangles in Fig. 15. For example for $\phi_s = \delta = 90^0$, the number of events in the A_1^+ and A_1^- channels is 53 and 29, respectively, after allowing for the 10% relative detection efficiency of D_{CP} to D^0.

The procedure used is to perform many "experiments" starting with initial central values of 800 and 20 events for the A and $\bar{A}$ channel for specific values of ϕ_s and δ. Then we allow all measured event numbers to fluctuate statistically around their central values. The distribution in $\sin\phi_s$ for several choices of ϕ_s and δ is shown in Fig. 17. Taking r.m.s. values of $\sigma(\sin\phi_s) < 0.16$ as necessary for the observation of CP violation, the potential "discovery" region is shown in Fig. 18.

To be able to discover CP violation using this method requires a detector which has similar (but hopefully better) photon and charged particle reconstruction capabilities as CLEO II, excellent charged particle identification, and excellent vertex detection. The former two are important to increase the discovery potential or guard against smaller branching ratios. The latter two are necessary to reject backgrounds in these rather small signal samples.

It is not clear that particle identification and vertex detection will be sufficient to reduce the background to the required level. Examination of current CLEO data reveals that the equivalent branching ratio of the background in the $D^0\pi^-$ and $D^{*0}\pi^-$ signal regions is $\sim 10^{-3}$; this is large compared to the $\sim 18\times 10^{-6}$ branching ratio we are attempting to measure in the A channel. However, the particle identification of the current CLEO II detector is minimal for these final states and there is no vertex information on the D^0 or the B. On the other hand, low background levels are possible, being almost non-existent in the ψK^- final state. If the background from fake D^0 and non-K^- combinations could be eliminated, we would still be faced with the problem of the background from real $\bar{D}^0K^-$ combinations in continuum events.

Rate asymmetries

Any final state which can be produced with two different amplitudes can show CP violating effects. For example, it is possible for a "penguin" amplitude to interfere with a "tree" level amplitude. The measurement consists of finding a different number of events of B^- versus B^+ events. For example, one could search for an asymmetry, A, in the conjugate decay modes $K^-\pi^0$ and $K^+\pi^0$ where

$$A = \frac{N(K^-\pi^0) - N(K^+\pi^0)}{N(K^-\pi^0) + N(K^+\pi^0)}$$

In B^- decays the final states could be $K^0\pi^-$, $K^-\pi^0$, *etc.*.

The sample size for any particular mode is $N = N_{B\bar{B}}\mathcal{B}\epsilon$, where $\mathcal{B}$ is the branching ratio and ϵ is the detection efficiency. The total number of $B\bar{B}$ events required to get an s standard deviation effect in one mode is $N_{BB} = s^2/\mathcal{B}A^2\epsilon$. Provided that there is at least one mode with $\mathcal{B}\epsilon > 2\times 10^{-5}$ and $A > 20\%$, an integrated luminosity of 20 fb^{-1} would be sufficient to establish CP violation to 4 standard deviations.

Angular correlations in vector-vector decay modes

When there is a decay into two vector mesons, and if two amplitudes contribute, then it is possible for CP violation to be observed in differences between the angular distribu-

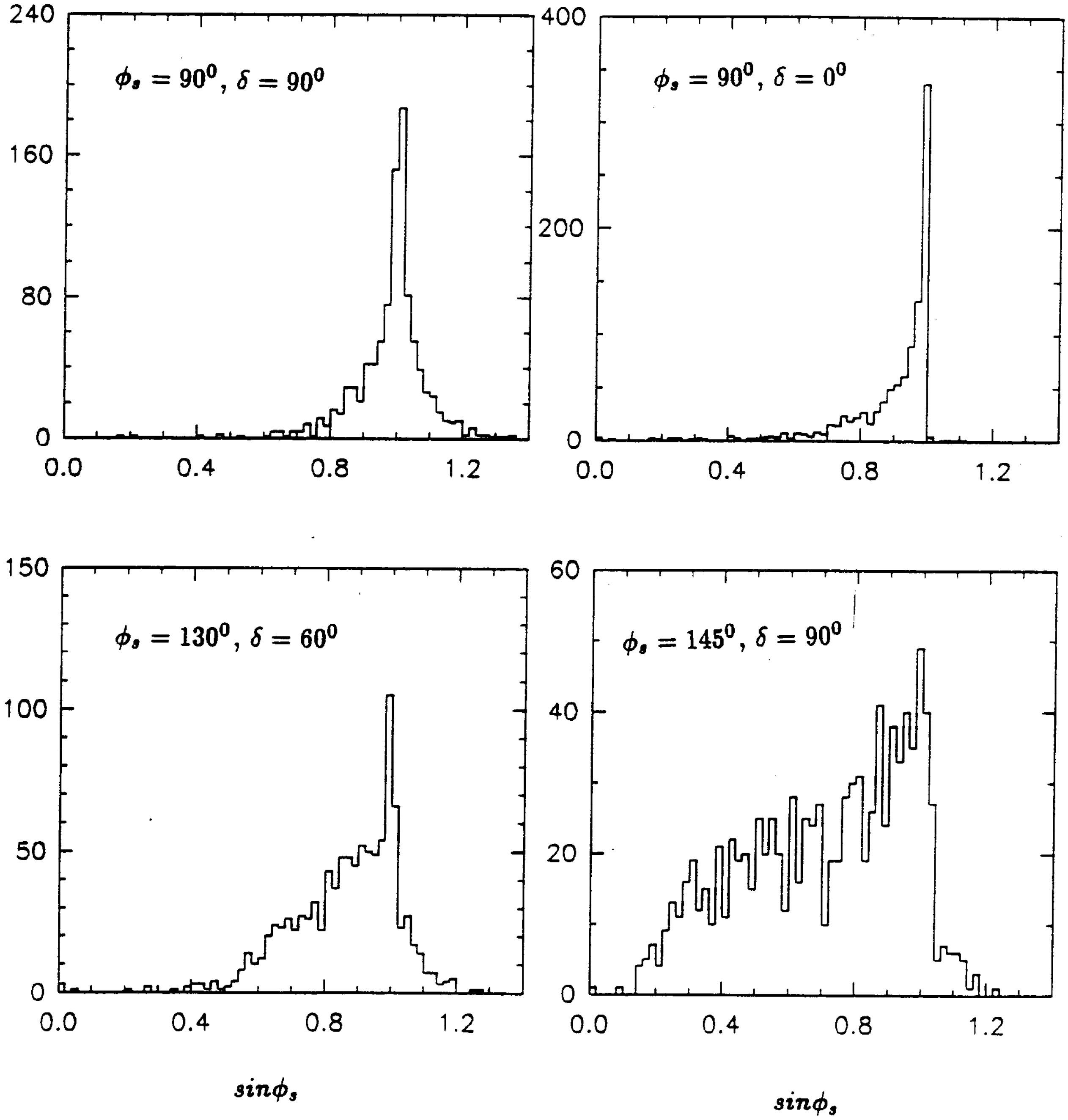

Figure 17: Values of $\sin \phi_s$ found for 1000 experiments and different input values as specified.

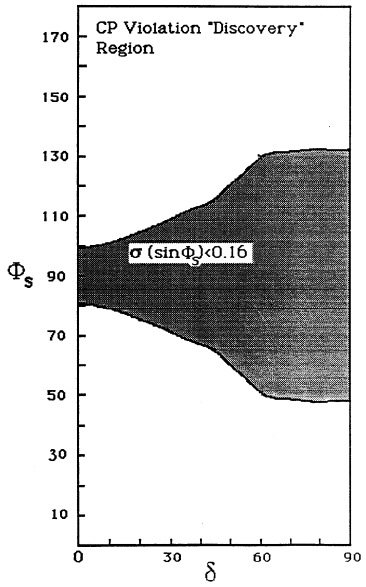

Figure 18: Region in $\phi_s - \delta$ plane of possible discovery of CP violation in 20 fb^{-1}.

tions of the B and $\bar{B}$. One way of looking for these asymmetries has been suggested by Valencia[44]. Defining the decay in terms of the momentum and polarization vectors as $B \to V_1(\mathbf{k}, \epsilon_1)V_2(\mathbf{q}, \epsilon_2)$, one can look directly at several asymmetries for both the B and the $\bar{B}$. For example

$$A_B = \frac{N(\mathbf{k} \cdot \epsilon_1 \times \epsilon_2 > 0) - N(\mathbf{k} \cdot \epsilon_1 \times \epsilon_2 < 0)}{N_{Total}},$$

is defined for the B decay and a similar quantity, $A_{\bar{B}}$ defined for the $\bar{B}$ decay. A difference between A_B and $A_{\bar{B}}$ would be evidence of CP violation.

Predictions of angular asymmetries in many channels such as $K^{*-}\omega$ have been given by Kramer and Palmer[46]. The predictions are quite sensitive to hadronic phase shifts. Therefore, it is difficult to make quantitative predictions, but such effects should be explored.

CP-odd energy asymmetries

It has been suggested by Burdman and Donoghue that CP violation might show up in three body decays modes, accessible from both B^0 and $\bar{B}^0$ decays, in Dalitz plot asymmetries[47]. One possible mode is $B \to K_S\pi^+\pi^-$. A distribution of interest is the shape of the summed energy spectrum of the π^+ and π^-. The average energy distribution can be written as $\langle E_\pi \rangle = a + b(E_{\pi^+} - E_{\pi^-})$. Finding that $b \neq 0$ is a manifest observation of CP violation. Again, there are no quantitative predictions.

2.2 Charm decay physics

The opportunities for performing charm physics studies at a high luminosity e^+e^- collider at a center-of-mass energy around 10 GeV are enormous especially when photons or π^0's are involved. Just below B meson threshold, $c\bar{c}$ events account for $\sim 40\%$ of the total cross section. Thus an integrated luminosity of 10 fb^{-1} will yield $\sim 2\times 10^7$ charmed particles. On the $\Upsilon(4S)$ which decays to B mesons, most of the B's decay to charmed particles increasing the yield further. This plus the excellent efficiency and resolution of the CsI calorimeter allows CLEO II and, therefore, CLEO III, to compete successfully with Fermilab fixed target experiments in situations where photon detection is important.

2.2.1 Semileptonic decays

Cabibbo-suppressed semileptonic decays provide an exciting laboratory for studying charm decays. These decays provide information on the ratio of CKM elements V_{cd}/V_{cs}. For decays to the vector final states, $\rho(\omega)\ell^+\nu$, measurement of the form-factor ratios can be related directly to the same final states in B decays which can allow extraction of V$_{ub}$ from $b\to u$ decays.

Already, the decays $D\to K(K^*)\ell\nu$ and $D^+\to\pi^0\ell^+\nu$ have been observed in CLEO II[48] and are providing important information on the form factors in charm decay. The approach is to use the decay chain $D^{*+}\to\pi^+D^0$ or $D^{*+}\to\pi^0D^+$ as a means to tag the D^0 or D^+ and to reduce background. Presently, the $D^0\to K^-\ell^+\nu_\ell$ data sample is the largest in the world and a clean signal $D^+\to\pi^0\ell^+\nu_\ell$ has been observed. Other Cabibbo-suppressed decays are obscured by their Cabibbo-favored counterparts. The $\pi^0\ell^+\nu_\ell$ signal is shown in Fig. 19 and is compared with the similar final state $K^0\ell^+\nu$. From these two signals CLEO finds V_{cd}/V_{cs}=0.21$\pm$0.02$\pm$0.02, where the second error results from the theoretical uncertainty in the value of the form-factor ratio at zero momentum transfer. Extending the semileptonic decay studies to the rarer ρ and ω final states requires excellent π^0 tagging efficiency and high luminosity, both of which will be available to CLEO III.

2.2.2 Hadron spectroscopy

HQET provides a wealth of predictions concerning the spins and decay patterns of charmed mesons and charmed baryons. Both will be copiously produced in CLEO III. Precision measurements of mass differences[49] may be used to determine the decay constant f_D[50]. Presently the D^*-D mass difference errors are of the order of 0.1 MeV/c^2. The CLEO III data sample of such decays should be more than an order of magnitude larger than that shown in Fig. 20 which comes from CLEO II.

CLEO III will thus provide the opportunity to measure the branching fractions, identify the excited states, and unravel the complexities of the weak decays of the D_s, Λ_c, Ξ_c^0, Ξ_c^+, and Ω_c mesons. This program for the D^0 and D^+, which took approximately 15 years, is only now nearing completion.

The study of excited vector states (*e.g.,* D^{**}) usually means fitting decay angular distri-

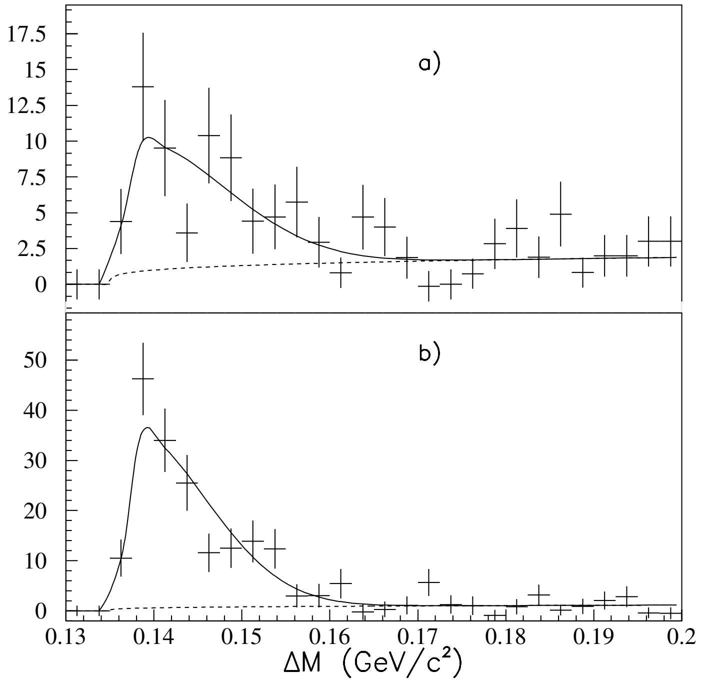

Figure 19: The D^{*+}-D^+ mass difference distributions, ΔM, for the candidates (a) $D^+ \to \pi^0_{fst}\ell^+\nu$ and (b) $D^+ \to \bar{K}^0\ell^+\nu$. The dashed curves are fits to the background and the solid curves are fits to the data including signal and background.

butions, and hence requires an extremely large data sample. Such studies will be possible in CLEO III providing an opportunity to make stringent tests of QCD models of the spectroscopy of mesons containing one heavy quark.

Spectroscopy has historically yielded surprises and the high statistics data sample of CLEO III will make it an ideal place to search for qg bound states, glueballs, and other exotica.

2.2.3 Rare charm decays

The separated vertices for charm mesons together with precise vertex location, excellent particle identification, and excellent π^0 reconstruction make it possible to reduce backgrounds and study rare decay modes not accessible in other experiments. One example is the doubly Cabibbo-suppressed decay $D^0 \to K^+\pi^-$. Without good (4σ) particle identification this process is not easily separated from the background process $D^0 \to K^-\pi^+$.

Other rare decays provide a unique opportunity for looking beyond the Standard Model. Flavor-changing neutral currents, manifested by the decay $D \to X\ell^+\ell^-$, should exist and may have branching fractions of the order of 10^{-6}. Present limits by CLEO II are of the order of 10^{-4}.

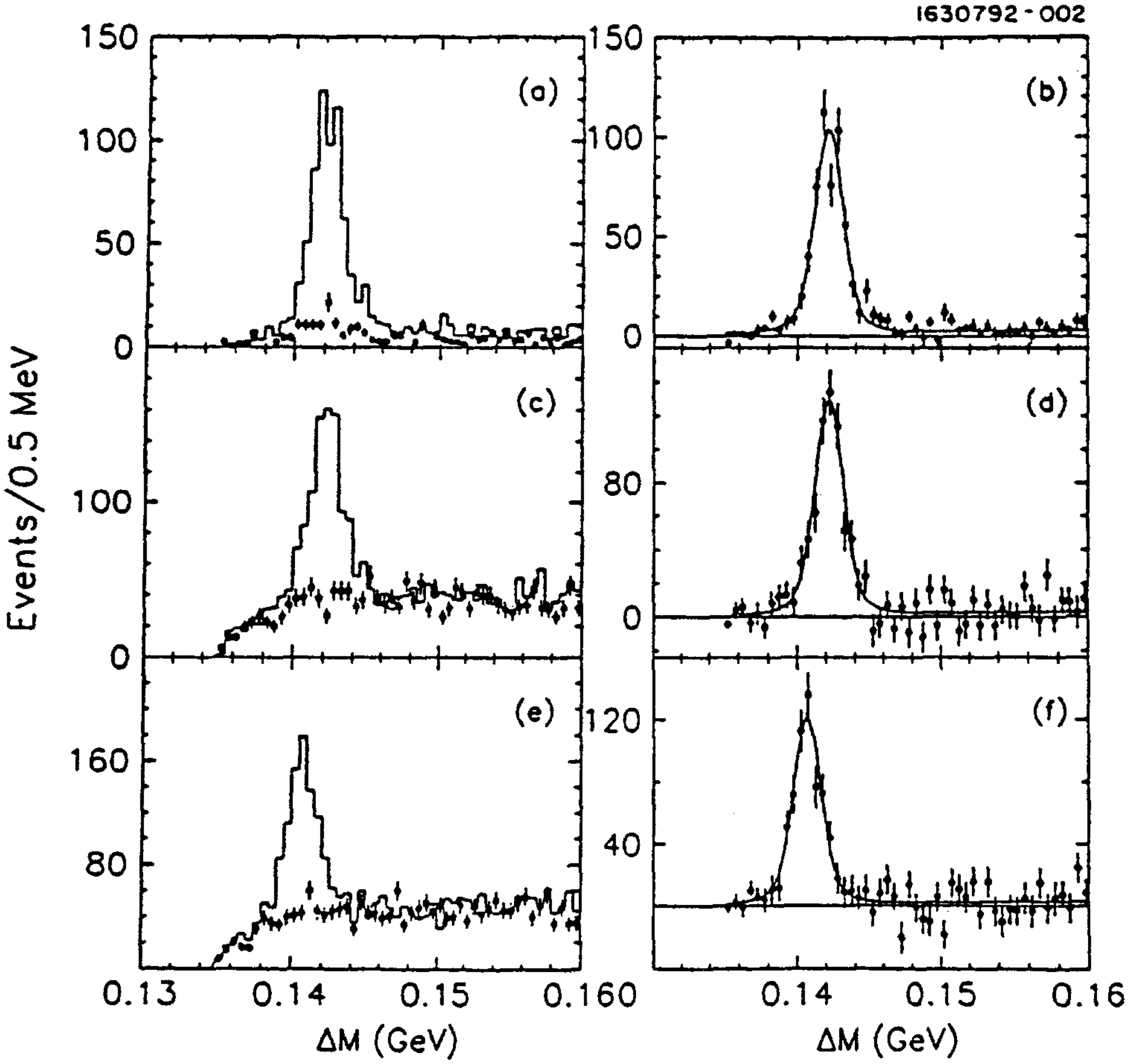

Figure 20: The $D^* - D$ mass difference distributions (ΔM) for (a) $D^{*0} - D^0$ with $D^0 \to K^-\pi^+$, the histogram shows the data cut on the D^0 mass, while the solid points show the sidebands. In (b) the sideband has been subtracted and the data fit to the signal plus plus background shapes described in the text; (c) and (d) are for $D^0 \to K^-\pi^+\pi^0$ and (e) and (f) show the $D^{*+} - D^+$ mass difference with $D^+ \to K^-\pi^+\pi^+$.

2.2.4 Measurement of f_{D_s}

Of special importance is the purely leptonic decay $D_s^+ \to \mu^+\nu$. Measuring the width of this reaction determines the decay constant f_{D_s}. This decay constant can be calculated theoretically as can the decay constant f_B. In fact, lattice gauge calculations have made estimates of both numbers. Knowledge of f_B is crucial in testing Standard Model parameters. It is, in fact, very difficult to measure f_B directly since the purely leptonic decays needed to measure it directly proceed through the $b \to u$ channel and have extremely small branching ratios. It is possible, however, to measure f_{D_s} through its dominant $c \to s$ decay channel. CLEO II has made the first measurement of the ratio $\Gamma(D_s^+ \to \mu^+\nu)/\Gamma(D_s^+ \to \phi\pi^+ {=} 0.25 \pm 0.03 \pm 0.07$, using D_s's tagged by the decay $D_s^* \to \gamma D_s$[51]. In order to extract a value for f_{D_s}, the value of the $\phi\pi^+$ branching ratio must be known. Using an estimate relating D_s semileptonic decays to D^+ semileptonic decays, CLEO II finds $f_{D_s} = (344 \pm 37 \pm 52 \pm 42)$ MeV. The last error is due to the uncertainty on the $\phi\pi^+$ branching ratio, $(3.7 \pm 0.9)\%$, which is consistent with more recent estimates[52]. CLEO III will be able to substantially reduce the errors on both the partial width ratio and the absolute branching ratio.

2.2.5 Charm mixing

Expectations for the $D^0\bar{D}^0$ mixing parameter range from $\sim 10^{-4}$ to 10^{-7} in the Standard Model[53]. Based on our present experience with CLEO II, we expect that sensitivities below 10^{-5} will be achieved with CLEO III. The most obvious method to detect such mixing is by observing the decay chain $D^{*+} \to D^0\pi^+, D^0 \to K\pi$. The sign of the π from the D^{*+} decay tags the decay as either a D^0 or $\bar{D}^0$; then the sign of the K indicates whether the D^0 has mixed before decaying. The main background comes from doubly Cabibbo-suppressed decays of the D^0 with a rate proportional to $\tan^4\theta_c{=}0.003$, which is measured to be much larger than the mixing signal[54]. Nevertheless, a good measurement of the time dependence should easily separate the two processes. The conventional doubly Cabibbo-suppressed decays should follow a $e^{-\Gamma t}$ while for mixed events the distribution is

$$e^{-\Gamma t}\left(1 - 2\cos(\Delta m t)e^{\Delta\Gamma t/2} + e^{\Delta\Gamma t}\right) \tag{13}$$

This measurement relies heavily on the vertexing capabilities of the silicon detector, on the angular resolution of the slow π, and on good π/K separation. A large value of the mixing parameter would indicate physics beyond the Standard Model.

2.3 Tau decay physics

Results from SLC and LEP indicate that there are only three generations of leptons[55] within the standard gauge theory of electromagnetic and weak interactions[56]. The heaviest of these leptons, the τ, serves as an excellent laboratory for studying many aspects of the

Table 7: Data sample for selected τ decay modes assuming an integrated luminosity of 30 fb^{-1}.

Decay Mode	Number of Events $\times 10^6$
All τ's	54
$\tau^- \to e^- \nu_\tau \bar{\nu}_e$	10.8
$\tau^- \to \mu^- \nu_\tau \bar{\nu}_\mu$	10.6
$\tau^- \to \pi^- \nu_\tau$	7
$\tau^- \to K^- \nu_\tau$	0.4
$\tau^- \to K^{*-} \nu_\tau$	0.9
$\tau^- \to \eta X^- \nu_\tau$	> 0.1
$\tau^- \to \omega X^- \nu_\tau$	1
$\tau^- \to K^- K^+ \pi^- \nu_\tau$	~ 0.13
$\tau^- \to$ 3 charged tracks	8
$\tau^- \to$ 5 charged tracks	0.06

Standard Model[57]. Of all the known leptons only the τ is massive enough to decay into both purely leptonic states and semileptonic states with accompanying hadrons. The purely leptonic decays allow the study of lepton universality and the $\tau - \nu_\tau - W$ vertex, while the semileptonic decays permit the investigation of the weak hadronic current and strong interaction effects. The decay of the τ allows the measuring of the ν_τ mass and the search for Standard Model forbidden decays involving three generations of leptons with or without accompanying hadrons.

To date all meaningful studies of the properties of the τ have been carried out at e^+e^- colliders. At these facilities the cross section for τ production is relatively large while the associated backgrounds are both calculable and small. These advantages suggest that e^+e^- colliders will be the place to measure the decay characteristics of the τ for many years to come. For CLEO III we assume an integrated luminosity of 30 fb^{-1} for which there will be about 27 million τ pairs produced. In Table 7 we list the data samples which will be available for various τ decays. In this section, we discuss a selected sample of physics topics that can be studied at an upgraded CESR/CLEO facility. We will assume that the one-charged-particle decay discrepancy has been resolved and thus will not be discussed here.

2.3.1 Tau neutrino mass

The Standard Model has no predictive power on the neutrino masses. However, a non-zero neutrino mass is predicted in many of the fashionable extensions of Standard Model such as compositeness, Grand Unified Theory, and the left-right symmetry model[58]. A sufficiently massive neutrino is also a popular solution to the solar neutrino and dark matter problems. Since there are only three generations of leptons, ν_τ is the only potential candidate to solve these problems. The upper limit on the mass of ν_τ is 31 MeV/c^2 at 95% confidence level[59]; for comparison, the mass limits on ν_e and ν_μ are 17 eV/c^2 and 270 KeV/c^2, respectively[42]. In some models, an assumption is made for the mass hierarchy

$$m_{\nu_\tau} = m_{\nu_e} \times \left(\frac{m_\tau}{m_e}\right)^2 \quad .$$

Given $m_{\nu_e} = 17$ eV/c^2, m_{ν_τ} is expected to be 206 MeV/c^2. Therefore, the limit on m_{ν_τ} already exceeds the sensitivity of ν_e and ν_μ limits in these models. A sensitivity to m_{ν_τ} of 3 MeV/c^2 corresponds to a sensitivity of 0.25 eV/c^2 on m_{ν_e}. Measuring the τ neutrino mass, therefore, can be a sensitive probe of the phenomenon of neutrino mass.

The best probe of τ neutrino mass is the shape of the end-point mass spectrum of the hadronic decay products. One of the decay modes with sensitivity to m_{ν_τ} is $\tau^- \to \pi^-\pi^+\pi^-\pi^+\pi^-\nu_\tau$. In general, the mass spectrum of the hadronic system depends on the unknown intermediate resonance structure. Fortunately, the end-point mass spectrum[60, 61] in this decay is dominated by the weak decay matrix element $\mathcal{M}$ and the phase space factor Φ,

$$\frac{d\Gamma}{dm} \propto m\mathcal{M}^2\Phi \quad ,$$

where m is the mass of the hadronic system,

$$\mathcal{M}^2 = (m_\tau^2 - m^2)(m_\tau^2 + 2m^2) - m_{\nu_\tau}^2(2m_\tau^2 - m^2 - m_{\nu_\tau}^2) \quad ,$$

and

$$\Phi^2 = [m_\tau^2 - (m + m_{\nu_\tau})^2] \times [m_\tau^2 - (m - m_{\nu_\tau})^2] \quad .$$

The candidates for $\tau^- \to \pi^-\pi^+\pi^-\pi^+\pi^-\nu_\tau$ can be selected with an e or μ tag with no photon above a certain threshold energy. Based on the experience with CLEO II, we expect a detection efficiency of $\sim$ 15%. For a data sample of 3×10^7 $\tau^+\tau^-$, this corresponds to at least 2000 events in the final sample which allows the detailed examination and fitting of the full mass spectrum. This is much more satisfactory than previous methods which are dominated by the highest mass event (which may actually be background). With the expected mass resolution of $\sim$ 10 MeV/c^2, the sensitivity on m_{ν_τ} is a few MeV/c^2.

While $\tau^- \to \pi^-\pi^+\pi^-\pi^+\pi^-\nu_\tau$ has historically been the favored decay mode to probe m_{ν_τ}, there are several other candidate reactions which may play an important role in this area that are accessible with the detector upgrades proposed here. In Table 8 we list several of these modes. In particular, the mode $\tau^- \to K^-K^+\pi^-\nu_\tau$ is attractive due to the large minimum hadronic mass in the decay. At the present time the CLEO experiment is unable to use this mode as it lacks the necessary particle identification. A phase space Monte Carlo of $\tau^- \to K^-K^+\pi^-\nu_\tau$ shows that only $\sim$1% of the decays have both kaons in the momentum interval $p < 0.8$ GeV/c where kaons can be unambiguously identified in CLEO II. Raising the momentum cutoff to 3 GeV/c in CLEO III improves the acceptance to 90%. Thus with the proposed CLEO III improvements in high momentum kaon identification, the mode $\tau^- \to K^-K^+\pi^-\nu_\tau$ will compete with $\tau^- \to \pi^-\pi^+\pi^-\pi^+\pi^-\nu_\tau$ as the standard channel to use for measuring m_{ν_τ}.

Table 8: Candidate τ decay modes for measuring m_{ν_τ}.

Decay Mode	Branching Ratio $\times 10^{-3}$	Minimum hadronic mass (GeV/c^2)
$\pi^-\pi^+\pi^-\pi^+\pi^-$	0.6	0.7 or 1.68^{ab}
$\pi^-\pi^+\pi^-\pi^+\pi^- n(\pi^0)$	1.1	0.7
$\pi^-\pi^+\pi^-\pi^0\pi^0$	$\sim$4.8	0.7 or 1.07^c
$K^-K^+\pi^-$	$\sim$2.2	1.13
$K^*(890)K^- n(\pi^0)$	3.2	1.39^b

^{a} assuming $\rho^0\rho^0\pi^-$ dominates.

^{b} must take into account resonance width.

^{c} for $\omega\pi^-\pi^0$ submode.

2.3.2 Decay modes and branching ratios

The partial widths for most of the τ decay modes can be calculated with the present understanding of the Standard Model. The purely leptonic decays can be calculated rigorously, including radiative corrections. Most of the major semileptonic decays with accompanying hadrons can be calculated reliably using experimental data such as π and K decay constants and the cross section of e^+e^- annihilation into hadrons. Since some of the semileptonic decays cannot be calculated accurately, the total decay width is unknown. It is therefore customary to express the branching ratios normalized to the electron branching ratio $\mathcal{B}_e$. Alternatively, the dependence on $\mathcal{B}_e$ can be eliminated by taking the ratio of two branching ratios. This is actually a preferred method of comparing the experimental measurement with the theoretical expectation because many systematic errors cancel in the ratio. In fact, some of the current experiments may be systematics limited after collecting data for a few more years. Since we do not expect any dramatic improvement in the systematic errors in the large data sample expected with the detector under discussion here, comparing the ratio is the only reliable method for the precision test of the prediction. In this section, we discuss the expected precision of the ratios. Also included is a discussion on the sensitivity on the highly suppressed second-class-current decay and the forbidden lepton-number-violating decays.

Tau decays to e and μ

In the Standard Model, the purely leptonic decays of the τ can be calculated rigorously, including the electroweak radiative corrections. This allows a precise test of lepton universality. The branching ratios for the two decays differ by a small phase space factor[60, 62],

$$\frac{B_\mu}{B_e} = 1 - 8y + 8y^3 - y^4 - 12y^2 \ln y = 0.973 \quad ,$$

where $y = (m_\mu/m_\tau)^2$. The current ratio is 0.988 ± 0.022[42].

At the present time the most precise measurement of the electronic branching fraction

$\mathcal{B}_e$ is from CLEO II using a data sample in which both τ's decay into electrons[63]. This ee analysis exploits the power of the CsI calorimeter and charged particle tracking system to reduce the backgrounds from radiative Bhabha and μ pair events to below 1%. A measurement of $\mathcal{B}_\mu$ using a similar technique is now in progress. Since the momentum of a μ candidate is required to be greater than $\sim$1 GeV/c for proper identification, the same momentum cut must be imposed on the e candidates for cancellation of the systematic uncertainties from tracking in $\mathcal{B}_\mu/\mathcal{B}_e$. Based on the CLEO II experience, we expect to obtain some 6×10^4 ee events and a similar number of $\mu\mu$ events from 3×10^7 τ pairs; this corresponds to a statistical precision of 0.28% on the ratio $\mathcal{B}_\mu/\mathcal{B}_e$. The background from other τ decay modes is expected to be less than a few percent and hadronic backgrounds are expected to be less than 1%, contributing equally to both samples. The overall systematic error in $\mathcal{B}_\mu/\mathcal{B}_e$ from the background corrections should be less than 0.1%. The other main source of systematic error is the detection efficiency which has two components: trigger and particle identification. The uncertainties in the e and μ identification efficiency do not cancel in the ratio because of the very different techniques involved. Detection efficiency uncertainty in the ratio could be known to 0.7% and this will dominate the overall precision.

An alternative method would use ρ *vs.* μ and ρ *vs.* e events to obtain $\mathcal{B}_\mu/\mathcal{B}_e$. This would likely reduce the systematic error due to more complete cancellation of various contributions, especially from trigger effects. We estimate our efficiency for such decay modes to be 15%, giving us some 4×10^5 of each type. The statistical uncertainty on $\mathcal{B}_\mu/\mathcal{B}_e$ in that case would be 0.22%. With either of these analyses, lepton universality, therefore, can be tested with much improved precision over current measurements.

Tau decays to π and K

The partial widths for the two pseudo-scalar decays, $\tau^- \to \pi^-\nu_\tau$ and $\tau^- \to K^-\nu_\tau$, can be calculated using the experimental measurements of the π and K decay constants, f_π and f_K. The ratio of the two partial widths is related by the Cabibbo angle θ_C with a phase space correction factor [60, 62],

$$\frac{B_K}{B_\pi} = \frac{\Gamma_K}{\Gamma_\pi} = \tan^2\theta_C \frac{f_K^2 (1 - m_K^2/m_\tau^2)^2}{f_\pi^2\ (1 - m_\pi^2/m_\tau^2)^2} \quad .$$

Therefore, a precise measurement of the ratio of the branching ratios allows an accurate determination of the Cabibbo angle in τ decay with high momentum transfer. At present, the ratio is known only to $\sim 30\%$[42].

The CLEO II detector is not well suited for the measurement of this ratio. An accurate measurement of $\mathcal{B}_K/\mathcal{B}_\pi$ requires good π/K identification at high momenta since the momentum spectrum of the K or π is relatively flat up to 5 GeV/c and $\mathcal{B}_\pi$ is about $17\times$ $\mathcal{B}_K$. A preliminary study of $\mathcal{B}(\tau^- \to K^-\nu_\tau)$ using one-prong tau decays (1 *vs.* K) finds only $\sim$ 43 events/fb^{-1} yielding a detection efficiency of 0.45% in CLEO II. The detection efficiency is reduced greatly because a momentum cut of $p_K < 0.7$ GeV/c is required to obtain a relatively background free sample of $\tau \to K\nu$ decays. Increasing the momentum acceptance of the kaon to 3 GeV/c in CLEO III would increase the efficiency by roughly an order of magnitude.

For a data sample of 3×10^7 $\tau^+\tau^-$ and improved particle identification at high momentum we expect to identify 1.2×10^4 K candidates. Based on our preliminary analysis, the expected background level in the sample is $\sim$ 1%. Assuming a similar detection efficiency for $\tau^- \rightarrow \pi^-\nu_\tau$, we expect 2×10^5 events. Thus, $\mathcal{B}_K/\mathcal{B}_\pi$ could be measured with a statistical precision of $\sim$ 1%, a dramatic improvement over the current world average measurement.

Tau decays to ρ and K^*

The decays $\tau^- \rightarrow \rho^-\nu_\tau$ and $\tau^- \rightarrow K^{*-}\nu_\tau$ involve the coupling of the weak vector current to $\rho(770)$ and $K^*(890)$, respectively. Measurements of the branching ratios allow studies of the hadronic weak current. $\mathcal{B}_\rho/\mathcal{B}_e = 1.32 \pm 0.05$. The Cabibbo-suppressed K^* decay is related[60] to the Cabibbo-favored ρ decay by

$$\mathcal{B}_{K^*}/\mathcal{B}_\rho = \tan^2\theta_C \cdot f \cdot \frac{g_{K^*}^2}{g_\rho^2} \quad .$$

where the factor f corrects for the differences in the available phase space,

$$f = \frac{m_\rho^2}{m_{K^*}^2}\frac{(1-m_{K^*}^2/m_\tau^2)^2(1+2m_{K^*}^2/m_\tau^2)}{(1-m_\rho^2\ \ /m_\tau^2)^2(1+2m_\rho^2\ \ /m_\tau^2)} \quad ,$$

g_ρ and g_{K^*} are the coupling strengths of the ρ and K^* to the vector current. The relationship between the two couplings depends on whether the SU(3) symmetry is exact or broken. If SU(3) were exact, then $g_{K^*} = g_\rho$ giving

$$\mathcal{B}_{K^*}/\mathcal{B}_\rho = 0.038 \quad .$$

On the other hand, for broken SU(3) the Das-Mathur-Okubo[64] sum rules give $g_{K^*}/m_{K^*} = g_\rho/m_\rho$ and the prediction becomes

$$\mathcal{B}_{K^*}/\mathcal{B}_\rho = 0.052 \quad .$$

The current world average measurement of the ratio is 0.061 ± 0.009, which excludes the exact SU(3) symmetry at $\sim 2.5\sigma$ level[42].

For the measurement of the ratio, $\mathcal{B}_{K^*}/\mathcal{B}_\rho$, the ρ and K^* candidates can be selected using events where one τ decays via $\tau \rightarrow e\nu\nu$ or $\tau \rightarrow \mu\nu\nu$. For a data sample of 3×10^7 $\tau^+\tau^-$, we expect to collect 6×10^5 ρ candidates for a detection efficiency of 15%. Traditionally, the K^* decay is identified with a detached vertex through the decay chain, $K^{*-} \rightarrow \pi^-K_s^0 \rightarrow \pi^-\pi^+\pi^-$. Including the branching ratio for the decay chain, the detection efficiency is expected to be $\sim$5%. This yields 1.7×10^4 K^* candidates, corresponding to a statistical precision of 0.8% on the ratio of branching ratios. The dominant background in the ρ sample is the 3% feed down from the decay $\tau^- \rightarrow \pi^-2\pi^0\nu_\tau$. In the K^* sample, we expect a contamination of 5% from the three-charged-pion decay. The background from the misidentification of π as a lepton tag has equal contributions to both samples. We expect an overall systematic error of 0.4% from the uncertainty in the background subtraction. Since the topology of the K^* decay is quite different from that of the ρ, the systematic errors in identification efficiencies do not cancel in the ratio. We expect a systematic uncertainty of 1.6% on the ratio of these efficiencies. This yields an overall precision on the ratio of 1.8%, allowing a sensitive test of the Das-Mathur-Okubo sum rules.

An independent method of measuring the ratio is to use the other decay channel $K^{*-} \to K^-\pi^0$. A preliminary analysis using CLEO II data where the K^- is required to have $p_K <$ 0.7 GeV/c yields 18 $\tau \to K^-\pi^0\nu$ candidates per fb^{-1} with about 20% background. The overall detection efficiency for this process is only $\sim$0.23% and is dominated by the limited momentum range of particle identification. Extending the π/K identification up to 3 GeV/c would increase the detection efficiency for this mode by a factor of 15. A similar gain in the purity of the sample is expected with improved particle identification. Thus, for a 30 fb^{-1} data set, we expect 4500 events providing a measurement of $\mathcal{B}_{K^*}/\mathcal{B}_\rho$ with a statistical precision of 1.5% and with much lower systematics than the previous method.

Tau decays with η mesons

CLEO has recently observed the first example of τ decays with an η meson in the final state, $\tau \to \pi^-\eta\pi^0\nu_\tau$[65]. The branching ratio for the decay has been calculated using the measured cross section for $e^+e^- \to \eta\pi^+\pi^-$ together with the CVC hypothesis. Using the cross sections measured at Novosibirsk and DCI, Gilman predicts[66] the branching ratio to be $\mathcal{B}_{\pi\eta\pi^0} = 0.15\%$. This is in good agreement with the CLEO II measurement of $(0.17 \pm 0.02 \pm 0.02)\%$.

There is no firm theoretical prediction on the branching ratio for the decay $\tau^- \to \pi^-\eta 2\pi^0\nu_\tau$. However, the branching ratio is related to that for the decay $\tau \to \pi^-\eta\pi^+\pi^-\nu_\tau$ by isospin invariance: $\mathcal{B}_{\pi\eta 2\pi^0} \leq \mathcal{B}_{3\pi\eta}$.

The decay $\tau^- \to K^-\eta\nu_\tau$ is allowed in the Standard Model but is suppressed. The branching ratio has been estimated using a Chiral Effective Lagrangian by A. Pich[67],

$$\mathcal{B}_{K\eta} \sim 1.2 \times 10^{-4} \quad .$$

There are other decay modes such as $\tau^- \to \pi^- 2\eta\nu_\tau$ and $\tau^- \to \pi^- 2\eta\pi^0\nu_\tau$ which are predicted to have very small branching ratios.

To study the above decays requires large data samples and these can only be observed and studied at a facility with CESR Phase 3 levels of luminosity and a detector comparable to CLEO III.

Second-class-current decay

The decay $\tau^- \to \pi^-\eta\nu_\tau$ is of particular interest in the Standard Model of electroweak interactions as it is an example of a decay via a second class current. Weak currents are classified according to their G parity as shown in Table 9.

Table 9: Classification of weak currents according to their G parity

Current Class	Vector	Axial Vector
First	$G=+1$	$G=-1$
Second	$G=-1$	$G=+1$

Since the final state contains two pseudoscalars, the decay must proceed by a vector current, but the G parity of the $\pi\eta$ is $G=-1$, hence this proceeds through a second class current. Second class currents are strongly suppressed due to isospin symmetry in the Standard Model and a branching ratio of order 10^{-5} is expected. Observation of a sizable branching fraction could indicate the existence of second class currents or some other new interaction. The current upper limit on this branching ratio is 3.4×10^{-4} at the 95% confidence level[65] and could approach 3×10^{-5} for CLEO II, but will likely be limited by background from $\tau\rightarrow K\eta\nu_\tau$ given the poor CLEO II π/K separation.

The simplicity of the decay process $\tau^-\rightarrow\pi^-\eta\nu_\tau\rightarrow\pi^-\gamma\gamma\nu_\tau$ provides a clean laboratory for the search[68]. The candidates for the decay can be selected with a lepton tag. A π tag with no accompanying photon may also be possible. The η meson is required to decay into the $\gamma\gamma$ final state. The other η decay channel, $\eta\rightarrow\pi^+\pi^-\pi^0$, is not usable because of the large background from the unsuppressed decay $\tau^-\rightarrow\pi^-\pi^+\pi^-\pi^0\nu_\tau$. The dominant backgrounds are expected to be due to the following decay modes:

- $\tau^-\rightarrow\pi^-\pi^0\nu_\tau$, where one of the photons from the π^0 decay is lost and the other photon is combined with initial state radiation or a fake photon created by the crystal clustering algorithm due to shower fluctuation or noise.
- $\tau^-\rightarrow\pi^-2\pi^0\nu_\tau$, where one photon from each π^0 decay is lost because the photon is very soft or merged with another photon.
- $\tau^-\rightarrow K\bar{\eta}\nu_\tau$, with the K misidentified as a π.

A special clustering algorithm optimized to reduce fake or merged photons may be required. The ability to detect (or veto) low energy photons will be crucial for suppressing these backgrounds. The last background should be manageable with the improved π/K separation of CLEO III. We expect a sensitivity to the branching ratio of order 10^{-5} for a data sample of 3×10^7 $\tau^+\tau^-$.

Forbidden decays

The search for decays forbidden by the Standard Model has long been a tradition of particle physics. In recent years the immense interest in models that go beyond the Standard Model, such as compositeness, technicolor, lepto-quark, and new horizontal gauge bosons, has intensified interest in these kinds of searches[69].

The traditional hunting ground, such as μ or K decay, has a limited number of decay channels because of the limited phase space. The τ lepton is an ideal laboratory for the search of the decay of a third generation lepton into first or second generation leptons or hadrons. The large lepton mass allows the decay into a number of purely leptonic final states such as $\tau^- \rightarrow e^-e^+e^-$ and $\tau^- \rightarrow \mu^-e^+e^-$ or semileptonic final states such as $\tau^- \rightarrow e^-K^0$ and $\tau^- \rightarrow \mu^-\rho^0$. In several interesting models the rate for a lepton number violating decay involving a τ is many orders of magnitude larger than a similar decay involving a muon due to the large mass of the τ. For example, in a superstring model τ decays are enhanced by $(m_\tau/m_\mu)^5$ over muon decays leading to the prediction that $\mathcal{B}(\tau \rightarrow \gamma\mu) \sim 2 \times 10^5 \mathcal{B}(\mu \rightarrow \gamma e)$. In a model with a charged Higgs, τ decays are enhanced by $(m_\tau/m_e)^2$ leading to the prediction that $\mathcal{B}(\tau \rightarrow \mu\mu\mu) \sim 2 \times 10^7 \mathcal{B}(\mu \rightarrow eee)$.

To date the most sensitive search for lepton number violating τ decays has been carried out by the CLEO II experiment. Here a 95% confidence limit of 4×10^{-6} has been set for the decay $\tau \rightarrow \gamma\mu$[70]. Other experiments have set limits on similar decays which are in the range of 10^{-3} to 10^{-5}[42]. Since almost all of these searches have been limited by statistics (*e.g.,* the CLEO II result on $\tau \rightarrow \gamma\mu$), we expect to reach the sensitivity of 10^{-7} for most channels with a sample of 30 fb^{-1}.

2.3.3 Structure of the $\tau - \nu_\tau - W$ vertex

The large data sample expected permits a detailed investigation of the structure of the $\tau - \nu_\tau - W$ vertex. The Michel parameter ρ has been measured with a precision of 7% using the decay $\tau^- \rightarrow e^-\nu_\tau\bar{\nu}_e$ and 8% using the decay $\tau^- \rightarrow \mu^-\nu_\tau\bar{\nu}_\mu$[71]. This is in sharp contrast to the precision of 0.3% in μ decay[42]. Current τ measurements of this quantity are limited by statistics. A large sample of τ events can be selected using a ρ tag where the momentum of the lepton must be as low as practical for particle identification. We expect to achieve a precision comparable to that obtained in the μ decay. Unlike the μ decay, however, the two leptonic decay modes of the τ permit a test of lepton universality.

The measurement of the ρ parameter consistent with 0.75 could still allow some admixture of V + A, scalar, vector, or tensor interactions. The most general Hamiltonian for the four-fermion point interaction has ten complex coupling constants, corresponding to 19 independent parameters and an arbitrary phase. In contrast to the τ lepton where only the ρ parameter has been measured, the weak couplings of the μ have been completely determined. It is not necessary to measure all 19 observables in order to determine the interaction. Fetscher, Gerber, and Johnson[72] have shown only five measurements are needed to describe the interaction:

- lifetime
- decay asymmetry parameters ξ and δ
- polarization parameter ξ'

- inverse τ decay cross section S for $\nu_\tau e^- \to \tau^- \nu_e$ with ν_τ of known helicity.

The lifetime measurement will be discussed in the next section. The decay asymmetry parameters ξ and δ of the daughter lepton with respect to the spin direction of the parent lepton can be measured using the fact that the spin of the two $\tau's$ produced in e^+e^- annihilation are strongly correlated[60]. The spin of the τ can be determined from the two-body decay modes. For example, if we assume a pure V $-$ A interaction in the decay $\tau^- \to \pi^- \nu_\tau$, the π^- is emitted preferentially parallel to the spin of the τ^-. The spin of the τ^- can be selected by requiring the momentum of the π^- to be in the region corresponding to the π^- being produced forward or backward in the center-of-mass of the τ^-. The polarization parameter measurement requires the analysis of the polarization of the daughter lepton which is not yet practical at any e^+e^- collider. The cross section for $\nu_\tau e^-$ scattering is even less likely to be measured in the near future since direct ν_τ scattering is yet to be observed. Fetscher[73] finds that ρ, ξ, δ, and even η, the "low energy parameter," can be measured to a statistical precision of a few percent with the data sample expected from CLEO III.

2.3.4 Tau lifetime

The τ lifetime provides a direct measure of the coupling strength of the τ to the charged weak current. In the Standard Model, the decay $\tau^- \to e^- \nu_\tau \bar{\nu}_e$ proceeds in perfect analogy to the μ decay $\mu^- \to e^- \bar{\nu}_e \nu_\tau$. Assuming $\mu - \tau$ universality of the weak coupling and that the τ neutrino is massless, the τ lifetime is related to the μ lifetime[60]. Neglecting corrections of $O(10^{-4})$, we have:

$$\tau_\tau = \left(\frac{m_\mu}{m_\tau}\right)^5 \tau_\mu B_e \quad .$$

The statistical precision of the lifetime measurement for a sample of N events is given by

$$P = \frac{1}{\sqrt{N}} \left[A + B \left(\frac{\sigma_v}{\beta\gamma c\tau} \right)^2 + C \left(\frac{\sigma_b}{\beta\gamma c\tau} \right)^2 \right]^{1/2} \quad ,$$

where σ_v is the error in a single decay length measurement, σ_b is the beam spread, and $\beta\gamma c\tau$ ($\sim 250\mu m$ at $\sqrt{s}$=10.5 GeV) is the average distance a τ travels before decaying. The constants A, B, and C depend on the event topology. For events with the 1 $vs.$ 3 topology, $A = B = C = 1$ while 3 $vs.$ 3 events have $A = 0.5$, $B = 2$, and $C = 0$. The first term in the above expression is due to the exponential nature of the decay process. In the second term, with the silicon vertex detector, we expect σ_v to be $\sim 150\mu m$. The third term in the above expression takes into account the finite extent of the beams. To minimize this term, we can either select the events in the vertical plane or use events where both τ's decay into three charged tracks (3 $vs.$ 3). The measurement using 3 $vs.$ 3 events is independent of the beam size ($C = 0$) as it is the distance between the τ's that is measured.

To date, the τ lifetime has been measured with a statistical precision of 2% by individual experiments[42]. With the CLEO III τ sample it should be possible to make several independent measurements of the lifetime each with statistical uncertainty below 1%. For example, using events where one τ decays into an electron or muon we expect a precision of $\sim$0.3% assuming a detection efficiency for this mode of 15%. From a similar analysis using 3 *vs.* 3 decays we expect a lifetime measurement with precision $\sim$0.5% assuming a 15% detection efficiency for this mode.

Systematic errors will most likely dominate the measurement of the τ lifetime. The systematic error in this measurement has several components including charged particle tracking, and uncertainty in the size, composition, and lifetime of the non-τ events in the sample. With the large data sample and improved tracking due to the silicon vertex detector, we expect that a systematic error below 1% is feasible.

2.4 Two photon physics

The high luminosity running of CESR Phase 3 and the superb vertexing, particle identification, and calorimetry of the proposed CLEO III detector provide a unique opportunity for the study of two photon reactions. Studies of collisions at very high energies will only be possible at LEP or a linear collider, but the two photon physics program of CLEO will be more than competitive in the medium energy regime. In addition, this program will complement future investigations at low energy electron-positron colliders and studies of low energy proton-antiprotron annihilation.

The current two photon physics program at CLEO may be divided into four main categories, all of which will benefit from the improved luminosity.

- Two photon production of meson-antimeson and baryon-antibaryon pairs.
- Two photon production of mesonic resonances.
- Two photon production of charmonia.
- Two photon production of gluonia (ggg or $gggg$) or exotic quark bound states ($q\bar{q}q\bar{q}$).

Over the past two years CLEO has obtained results for the two photon production of proton-antiproton pairs[74]. Measurements of this reaction, when extended to sufficiently high two photon center of mass energies W, provide a test of perturbative QCD. The recent CLEO results extend previous measurements to values of W well beyond 3 GeV. The results show a measured cross section that is larger than the perturbative QCD prediction by approximately a factor of five at low W. The data approach the QCD prediction at large W where the perturbative calculation is expected to yield more accurate predictions. A calculation assuming the excitation of “diquark” intermediate states, on the other hand, is much more successful at predicting the reaction rate at lower W.

More recently CLEO has identified charged pion and kaon pairs at values of W up to 5 GeV[75]. These results also provide a test of QCD, but because of the smaller number of quarks involved and the larger values of W, the prediction is less model dependent. With more luminosity the range of these QCD tests will be extended even further so that the predictions may be challenged more accurately.

The "diquark" calculation also predicts the rates for the production of strange baryon pairs. The large data sets proposed should allow for successful searches for the production of $\Lambda\ \bar{\Lambda}$, $\Xi\ \bar{\Xi}$, and $\Sigma\ \bar{\Sigma}$ pairs. Measurements of the rates for these reactions should yield considerable information on the "diquark" production mechanism.

The two photon widths of charmonium states provide tests of the charmonium model and, when measured precisely, also test the QCD correction to the two photon widths. In the search for charmonium we have found evidence for the two photon production of the χ_{c2} through its decay into a photon and a J/ψ, and have measured its two photon width[76]. The two photon production of the χ_{c2} has also been detected through its decay into four charged pions. Although these processes have been observed by earlier experiments, the two photon width of the χ_{c2}, nevertheless, remains somewhat controversial as all present studies are severely limited by the available statistics. It will be possible with a much larger data set to settle the question of the two photon width of the χ_{c2}.

Two photon production of the η_c has been measured through its decay into $K_S K^\pm \pi^\mp$, and $K^+K^-\pi^+\pi^-$. The two photon production of the η_c will prove to be an important laboratory for the study of this resonance. In particular, the relative branching ratios of the η_c will be measured to a precision of about 5%, far better than at present.

The search for gluonium has started by looking for the production of two photon produced all-neutral final states. In this search good use is made of the high resolution CsI electromagnetic calorimeter.

The three tensor resonances $f_2(1270)$, $a_2^0(1320)$, and $f_2'(1515)$ are observed at present in both neutral and charged final states. With increased statistics it will be possible to measure the resonance parameters to high precision, but more interestingly, the mixing angle in the tensor nonet will be extracted with a precision of a few percent.

The superb resolution of the calorimeter has enabled the reconstruction of several "all photon" final states including $f_2(1270) \to \pi^0\pi^0$ and $a_2(1320) \to \pi^0\eta$. With increasing luminosity, the unusual line shape of the $a_0(980)$ will be resolved well through the decay $a_0(980) \to \pi^0\eta$. In addition, searches for other scalar states will result in very restrictive upper limits on the two photon widths.

Previous experiments have observed associated production of vector mesons in two photon collisions. The production rates have evidenced many puzzling features which have led to speculation that exotic intermediate states are involved. However, except for the case of $\rho\rho$ production, all of the previous studies have been limited by the available statistics. CLEO III will be able to measure the production rates and decay spectra very well and set stringent upper limits on the previously unobserved final states $\omega\phi$ and $\phi\phi$.

The greatest challenge for the upgraded CLEO III detector will be maintaining an efficient two photon trigger. With the capabilities of the vertex detector for rejecting cosmic ray, beam-wall and beam-gas backgrounds, we have the promise of a high luminosity source of two photon events to probe QCD processes and study rare or exotic states.

2.5 Υ physics

It is almost certain that CESR will remain the premier laboratory for studies of $b\bar{b}$ bound states for the next decade. Potential models describing the quarkonium interaction have met enormous success in predicting mass splittings in the heavy Υ system. Results from CESR on the masses and widths of the vector Υ systems and the masses of the orbitally excited χ_b states have been able to provide direct verification of such model predictions.

However, the study of Υ spectroscopy is far from complete. Remaining physics objectives include:

1. Measurement of the $b\bar{b}$ D-state masses.
2. Measurement of the dipion transitions among the χ_b states.
3. Measurement of the radiative widths of the χ_b and χ_b' states with $J = 0$.
4. Measurement of the $h_b(^1P_1)$ and $\eta_b(1^1S_0)$ masses.
5. Determination of the partial waves present in the dipion decays of the $\Upsilon(2S)$ and $\Upsilon(3S)$ states.
6. Observation of two-body radiative decays of the Υ, giving information on possible glueball states.

Some of these analyses should yield positive results using resonant data taken before the upgrade to CLEO III. Those that do will almost certainly await confirmation from future data sets. Also, at the higher luminosities expected for the future, we do not exclude the possibility that a larger data sample may provide some as yet unanticipated results. In any case, the future Υ spectroscopy program at CESR promises to refine our understanding of the basic quark-antiquark interaction.

2.6 Conclusions

Important τ, charm and B physics results are guaranteed with 30 fb^{-1} and a significantly upgraded detector. We can make precision measurements of the CKM elements V_{cb}, V_{ub} and

V_{cd}. We can measure the form-factors in the semileptonic decays $B \to D^* \ell^- \bar{\nu}_\ell$ and $D \to \omega \ell^+ \nu$ over the entire q^2 range and it may be possible to find $B \to \rho\gamma$ and thus determine another side of the CP triangle. There is also the exciting possibility that we can see evidence of CP violation.